ACTA MONTANA IRSM AS CR (1999)
Series A No.14(114), 5–23

ANALYSES OF ACOUSTIC EMISSION AND UNDERGROUND TREMOR TIME SERIES FROM ROCKBURST HAZARDOUS AREAS OF OSTRAVA–KARVINÁ MINES

R.ČÍŽ**), J.HOLEČKO*) and V.RUDAJEV**)

*) OKD, DPB Paskov. a.s., 73921 Paskov

**) Institute of Rock Structure and Mechanics, AS CR, V Holešovičkách 41, 18209 Prague

ABSTRACT. When mining coalface No. 14736 at ČSA mine in Ostrava – Karviná (south part of upper Silesian basin — North Moravia, Czech Republic) bituminous coal district a number of methods and measures aimed to prevent triggering of rockbursts were introduced. These concern primarily applications of coal seam destress blasting, no break blasting in overburden and wetting of a coal seam. Improving blasting accuracy was based on data from geophysical survey and also test hole drilling in this district was assessed. The main geophysical methods were seismological (SL) monitoring and measuring of seismo–acoustic (SA) emission in coalface foreground. From data collected by these two methods a time series characterizing seismic activity in the coalface area were compiled. Mining technology was characterized by mining advance data and data regarding blasting in coal seams and also in overburden. All these data were jointly processed by a neural network, which had to be able to predict future seismic activity and especially to signal a possibility of strong events on basis of "learning capability" using part of the input data.

KEYWORDS: acoustic emission, seismological monitoring, statistical methods, neural networks, mining induced tremors — rockbursts

INTRODUCTION

In the period from 8.9.1995 to 31.7.1997 at
ing the coalface no. 14736 classified as a hazardous rockburst
degree (the highest), took place. In regard to this classification systematic seismo–acoustic measuring of this locality and also continuous seismological monitoring of the area was carried out.

The seismo–acoustic measuring network was assembled from 5 – 7 sensors positioning of which was changed in relation to coalface advance. One of the piezoelectric sensors was located always in overburden in a drill hole approximately 5 m long, other sensors were located in the coal seam (usually two at
sensors frequency bands were between 70 Hz and 2 KHz.

Seismic measurements were carried out in the 1 – 50 Hz frequency band. Data interpretation consisted primarily of monitoring the frequency variation
of recorded signals and seismic events; at

and also spatial focus migration were evaluated. Horizontal networks (Slavík et. al., 1989) allowed the focus to be located fairly accurately, in the order of tens of meters. The vertical component of focus location was hampered by a larger margin error but it relative appreciation of different elevations of recorded seismic events. Data collected formed a database on the basis of which the measures against tremors could be improved. These measures consisted of proper blasting techniques (improving location and time accuracy of coal seam distress blasting from a coalface and no break overburden blasting from entries), and/or had the tendency to limit the mining speed, or even to stop the work at the coalface. The objective of this work is to process the recorded data by methods of multichannel statistical extrapolation and improve forecasting of future seismic events.

Input Data Characteristics

a) Seismic Data

During the entire period 9280 events were recorded by the seismic network. It was proven that events do not

by energy release in time (Fig. 1). According to the pattern of energy distribution the entire period can be split into 5 stages. The length of these stages was always restricted by a strong seismic event. In the initial mining phase, i.e. during the first three stages, the energy distribution between the strong seismic events was generally homogeneous and independent of mining advance. This advance has changed from 0.5 m/day to 3 m/day (first stage), after that it reached 1.5 m/day (part of the third stage), later to 2.0 m/day.

During the fourth stage lasting from 12.10.1996 till 4.6.1997, despite

the mining speed was practically the same (2 m/day) there was an increase of seismic energy. Following mining cessation on 30.7.1997 a sudden drop of seismic energy was noticed (fifth stage), but 11 days later the strongest induced seismic event of $E = 1.7 \cdot 10^6$ J occurred. When the mining activity was over, the phenomena were located in the cave–in area.

For all stages the frequency of energy distribution (EFD) was determined, while for the fourth stage where the homogeneous distribution of seismic energy was not determined, this distribution was assigned for three partial intervals, characterized by a different $\mathrm{d}E/\mathrm{d}t$ gradient and by a different volume of total seismic energy distribution. Results of these analyses are shown at Fig. 2 and 3. Virtually all EFD have the same form, i.e. in areas with

number of events than

and from the specific energy, which had a characteristic

to higher energies the distribution can be described by a logarithmic negatively exponential relation (Holub, 1995; Holub and Veselá, 1995; Kalenda, 1996; Rudajev et. al., 1996):

$$\log(N) = a - b \cdot \log(E)\,.$$

It is known that the scope of this energy is indirectly proportional

energy value per event

tribution). This relation was experimentally confirmed; for example during the

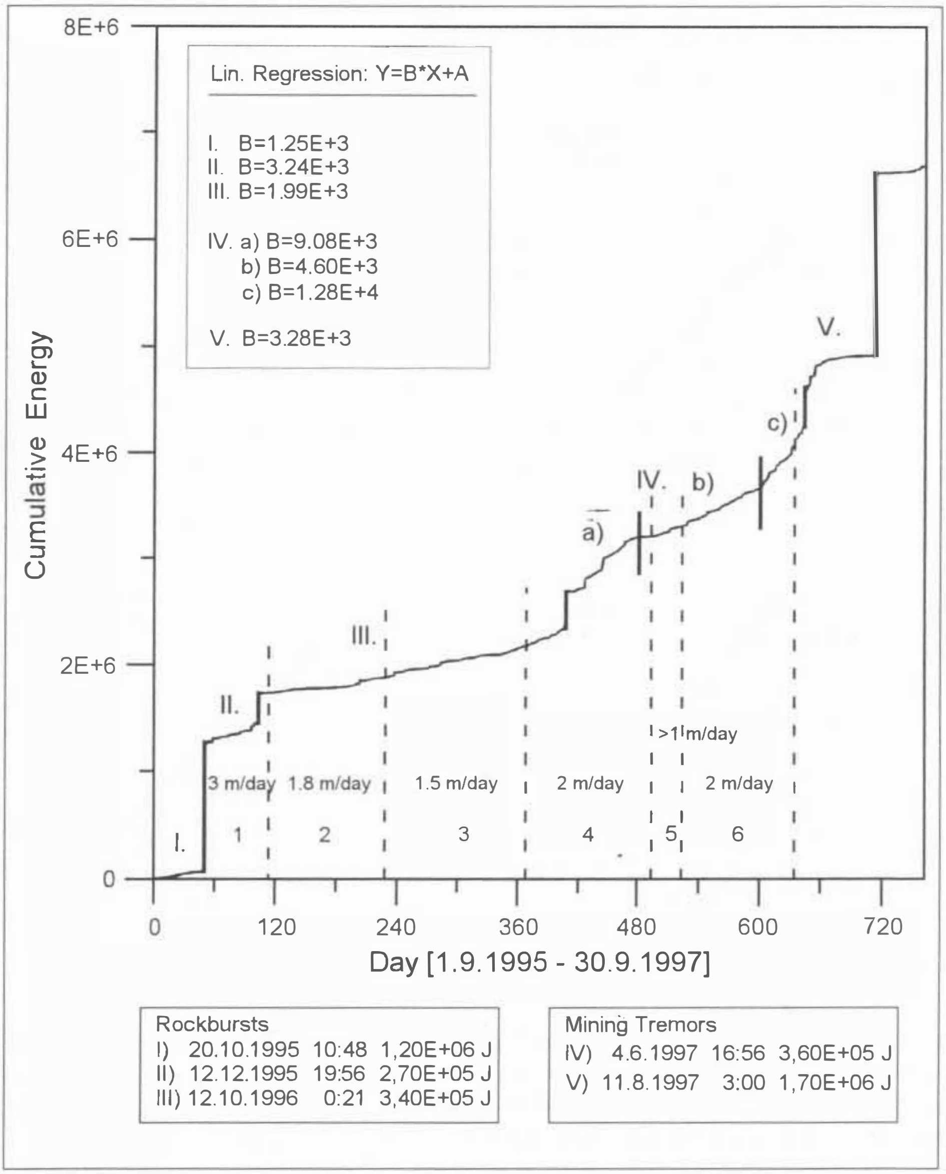

FIG. 1. Cumulative energy release, ČSA mine. Upper epochs I.–V. described seismic energy release between strong mining tremors. Lower intervals 1–6 described changes of average rate of mining

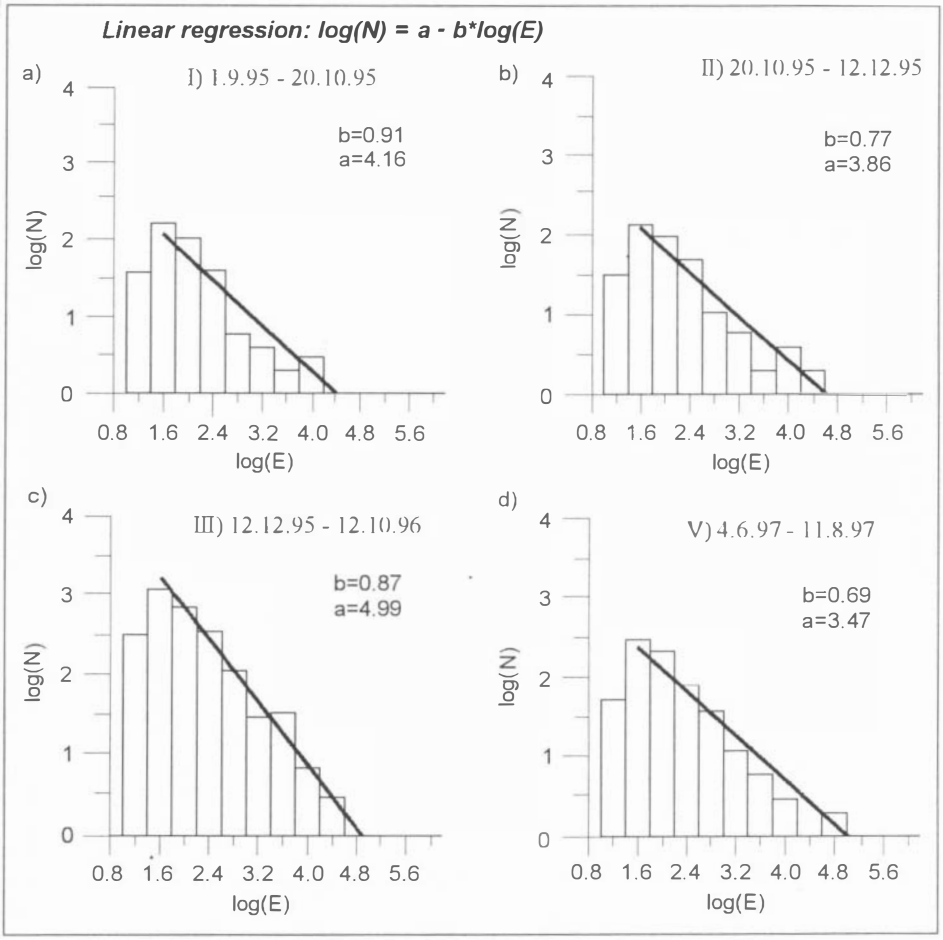

FIG. 2. Energy–frequency distributions for epochs I – III and V, ČSA mine

period when the seismic energy distribution was the lowest — first stage, where the mean energy value per tremor was 189 J — the slope of EFD was $b = 0.91$. On the other hand during the period of an increased seismic energy — fourth stage, interval c — the mean energy value reached 859 J and the gradient had a value of $b = 0.65$. These values formed a kind of integral characteristics process violation, but were not suitable for individual seismic event forecasting.

Locating of seismic events facilitated spatial monitoring of seismic activity development in the said area. Locations are shown in Fig. 4 where again the entire coalface mining period was divided in the stages defined above. From the focus distribution of the first stage it can be noticed that the seismic events were accumulated

seismic events directly related to the start of mining of coalface no. 14736. The second area of focus accumulation (the upper part of Fig. 4I) was evidently related to

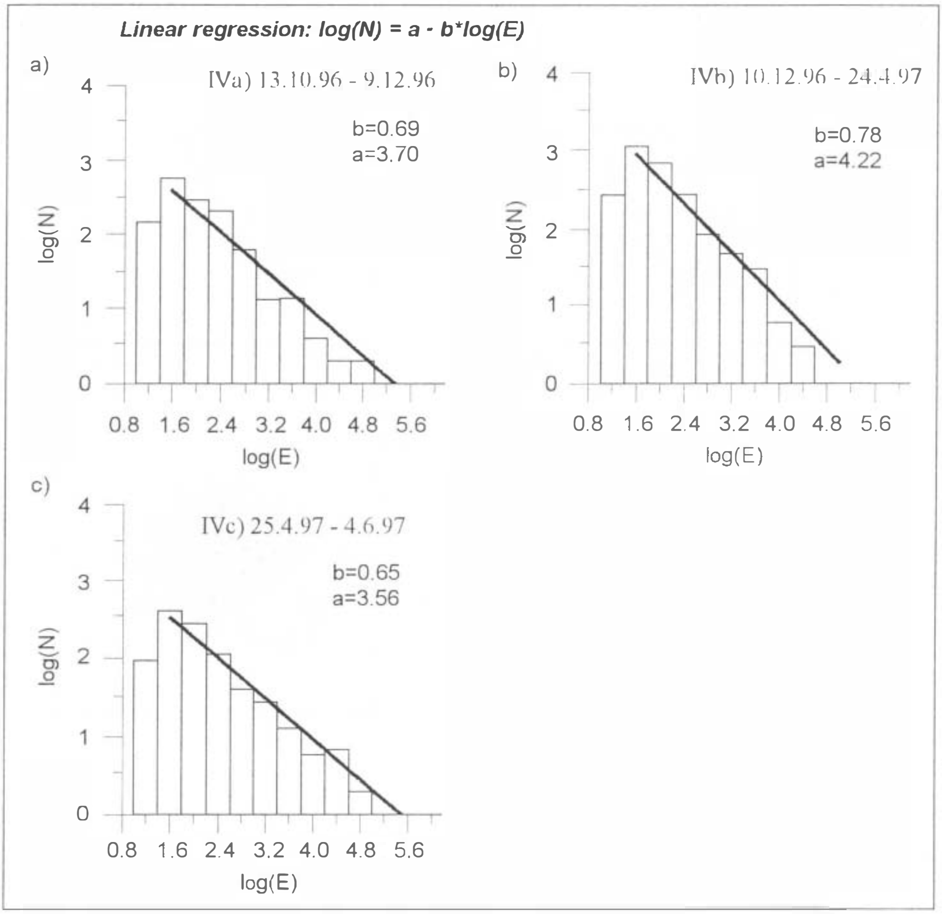

FIG. 3. Energy–frequency distributions for epoch IV, CSA mine

tl
neighbouring coalface and not
activity practically t
rheological processes in rock mass even after ending of mining activities. During the second and third stage of the currently
accumulation even some events related to previous mining activit
During the
area was under the influence of not recovered corner sections in overburden.

During the entire period 5 events in total were observed where energy exceeded 10^5 J. Three of these events could be classified as rockbursts, because they
microseismic effects
effect on mine workings. It can be assumed that it
the
events without any effects on mine workings with crosses.

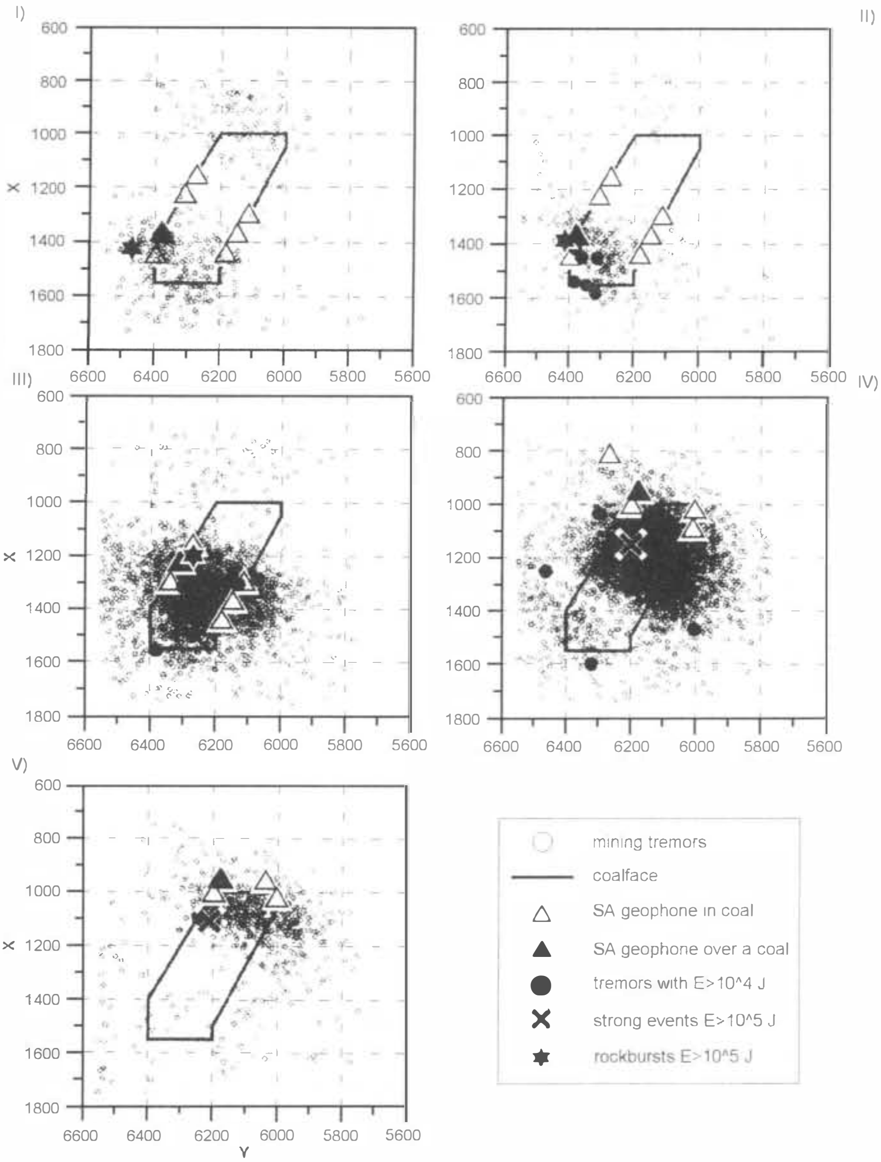

FIG. 4. Locations of mining tremors, ČSA mine, 1.9.1995 – 11.8.1997. Epochs I.–V. describe distribution of foci between strong mining tremors. Triangles show distribution of seismo-acoustic geophones.

b) Seismoacoustic Data

Seismic emission was monitored by 5 – 7 sensors moved according to mining activity. The monitoring system allowed
of their energy. Throughout the entire mining period 85000 seismo–acoustic pulses were recorded. From the location point of view the pulses were divided into pulses originating at coalface and pulses originating in overburden. Pulse frequency in time was not homogeneous.
technology and to induced seismic events. These aftershock sequences in particular helped to adjust the vertical component of seismic event focus more precisely. Fig. 4 shows typical configuration of sensors at individual stages marked with a blank triangle, sensor in overburden with a full triangle. Fig. 5 illustrates time curves of seismic energy distribution daily values
events (Fig. 5b), SA pulse number in the coal seam (Fig. 5c) and number of SA pulses triggered in overburden (Fig. 5d). Vertical dashed lines mark triggering of 5 strong seismic events in time. From the curve of SA pulse frequency in the coal seam and also in overburden it is obvious that the increase of pulses occurred only in case of the first (20.10.1995) and second (12.12.1995) rockburst. Concerning the remaining two strong events neither the precursor elements in the pulse frequency line, nor the number of seismically recorded events can be detected. This fact is obviously related to the bigger distance of the focus from mine working (higher-overburden). The hypothesis corresponds with the fact that in the case of the fourth and fifth
of these events.
multichannel statistical methods.

c) Technological Procedure

It is known that induced seismic events are triggered b
natural causes.
spaces are created), it changes the distribution of the initial stress condition and at the same time produces mass dynamic loading during blasting. For this reason mining advance and amount of blasting agent was monitored.

The excavation concerned coalface mining with an approx. 220 m long working face and the total length of coalface mined was roughly 450 m. Total thickness mined of seam No. 37 averaged
mined was 2.5 – 3.0 m. Mining of coalface No. 14736 started 8.9.1995 and was completed on 31.7.1997. Consequently the coalface was active 464 working days and 324 404 tons of coal in total was mined out, which is almost 700 t/day
complexity of mining it was in the mining solution for keeping the working face and the overpass drift No.14705/1, mined out almost parallel to the working face turning. From the mining point of view this area is characteristic for the cumulation different adverse impacts from previous mining activity like corner sections of not recovered overburden seams,
old shafts, abandoned mine workings of the neighbouring seam no.14730 etc. In the overburden (between

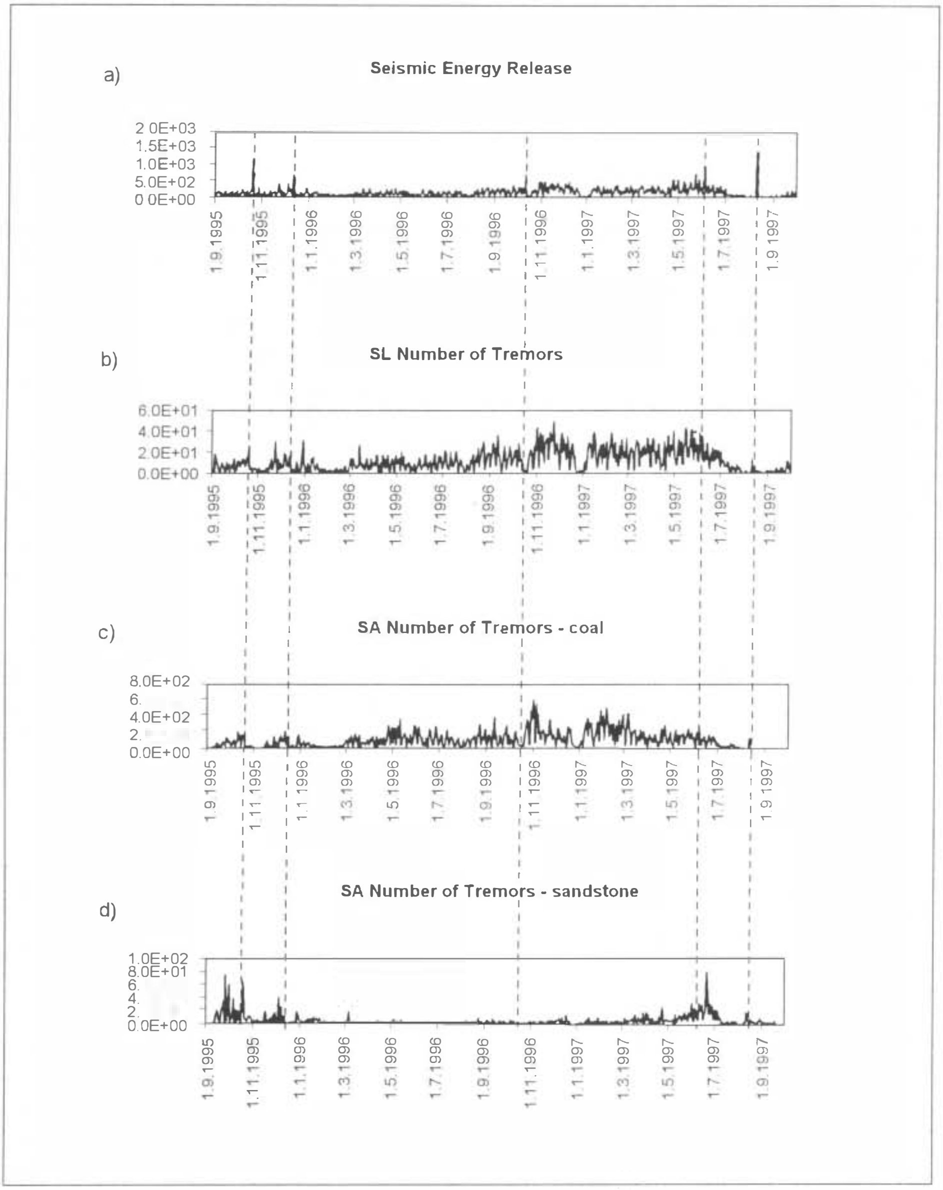

Fig. 5. Seismic (SL) and seismoacoustic (SA) time series of cumulative number of tremors per day and cumulative number of root square of seismic energy per day.

of up to
of strong overburden seismic activity, camouflet blasting
(BOS) with an impact effect of 30 m (vertical) at t
coalface foreground were implemented in advance. The BOS diagram is shown in Fig. 6a), where the amount of blasting agent used per day is shown. The average daily coalface advance
first two stages the advance
sometimes was not reached.

Methodology of Rockburst Occurrence Statistical Processing

The main objective of this work was to
for forecasting of induced seismic events. For this purpose the method of neural networks based on current processing of heterogeneous time sequences was applied and on the basis of determination of nonlinear relations between individual sequences it is possible to provide data extrapolation of the monit
This extrapolation was solved by a uniform network with an algorithm determining (learning) backpropagation with
ple that — it reaches
an optimal weight
Rudajev, 1996; R

$$\triangle w_{ij}^{(t)} = -\eta \frac{\partial E}{\partial w_{ij}} \left(\vec{w}^{(t)} \right) + \alpha \triangle w_{ij}^{(t-1)} .$$

where $\triangle w_{ij}^{(t)}$ are weight changes in iterative step t, $\frac{\partial E}{\partial w_{ij}} \left(\vec{w}^{(t)} \right)$ denotes gradient of energetic function, η is lea
phase
the requested paramet

For input
its energy, mining procedure and the
first stage
(Rudajev, Číž, 1998) was made.
be noticed that
SL events a 7 day
pulses recorded from overburden which proves that overburden does not respond to weekly working cycle. The same results were proven also in power spectrums.

During the analyses of SA and SL energy series (Fig. 8) it was found, that 7 day periodicity was displayed only by the series of SA energy released
(Fig. 9). Independence of the energy amount released from coal and overburden mass confirms the hypotheses regarding interaction of primary stress field of rock massif and its
vicinity of underground workings does not describe energetic changes in rock massif and therefore their contribution to
Because of the uncertainty of input set data the prediction of future events does not

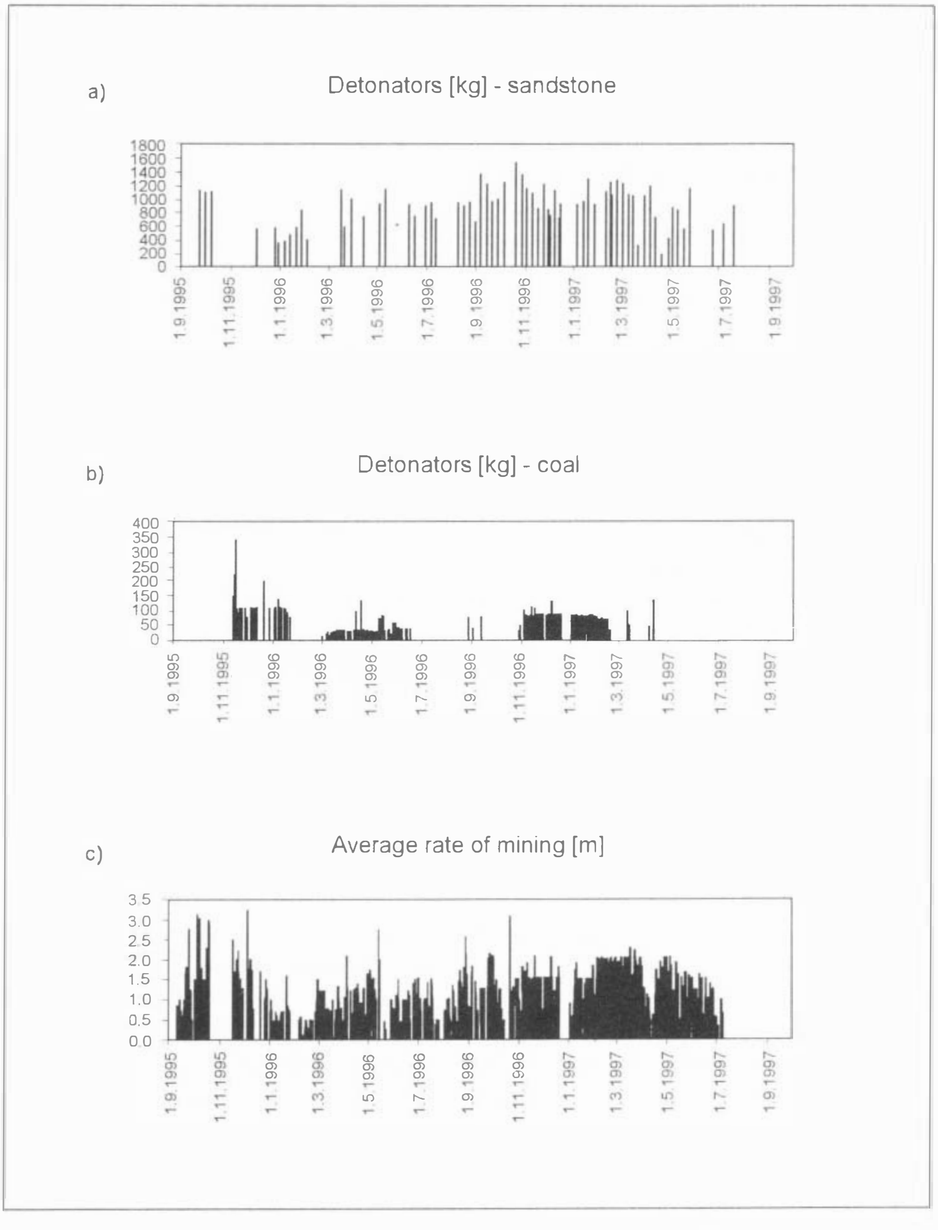

FIG. 6. Technological parameters: a) amount of blasts [kg/day] applied in sandstone, b) amount of blasts [kg/day] applied in coal, c) average rate of mining [m/day]

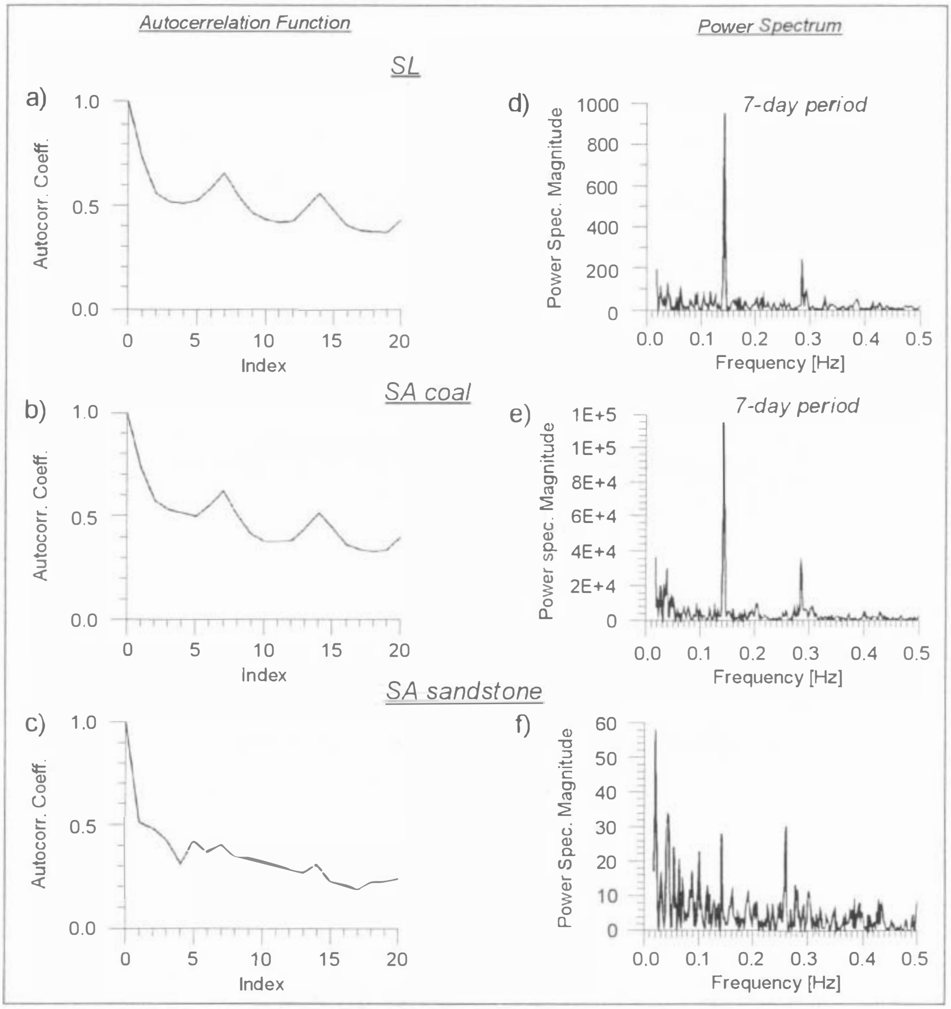

FIG. 7. Autocorrelation function and power spectral densities for seismic number of tremors (SL) and seismoacoustic (SA) number of tremors in the coal and in the sandstone over coal seam.

concern the time element of individual tremors but their total count or the total energy per day.

Input series were split into two parts — learning series included 600 succession elements and during this time 7332 events were recorded. For these "learning" series the parameters of neural network which included one hidden layer with three hidden neurons were determined. According to previous tests this appears sufficient (Rudajev, Číž, 1998). The prediction success rate was tested against the set of predicted values, which included 161 succession elements and was formed from

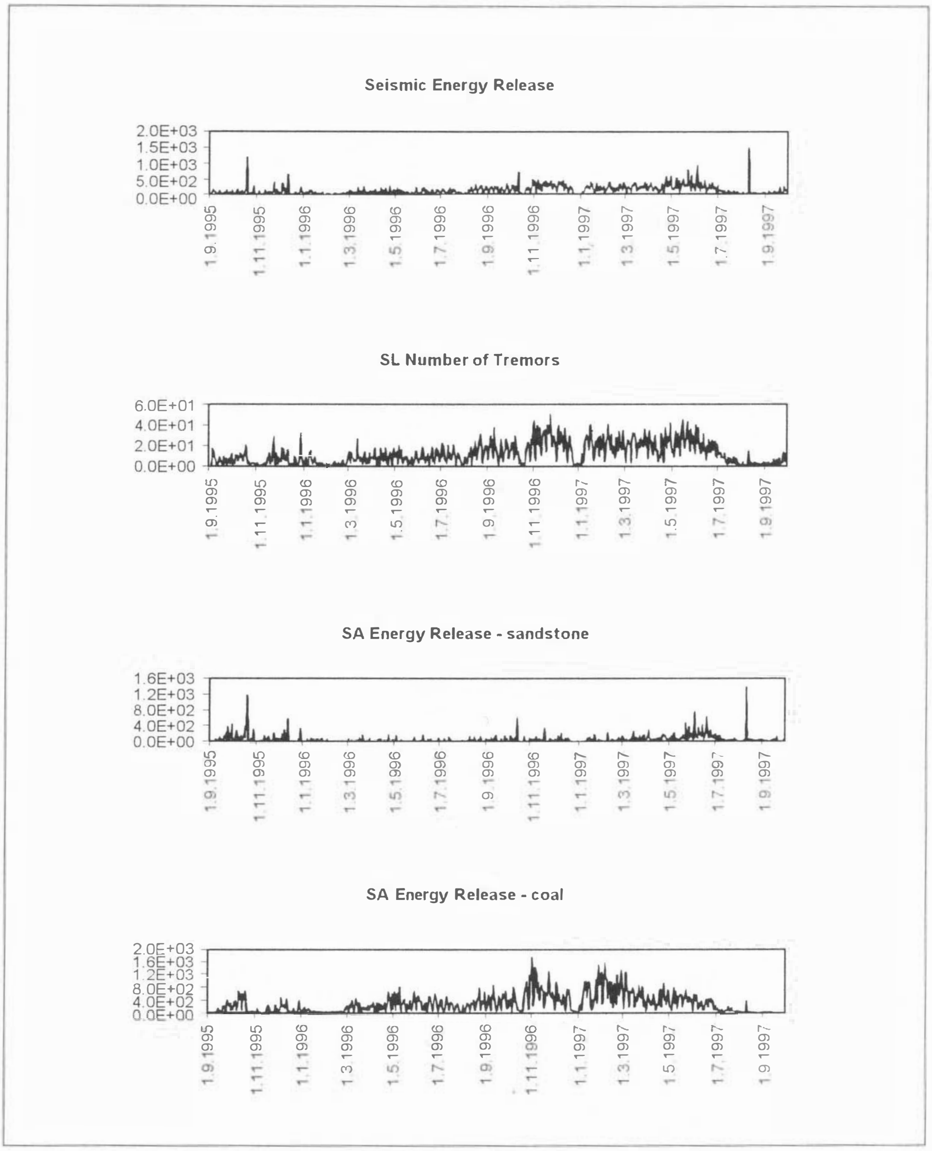

FIG. 8. Seismic (SL) and seismoacoustic (SA) time series of cumulative root square of seismic energy release and seismic cumulative number tremors.

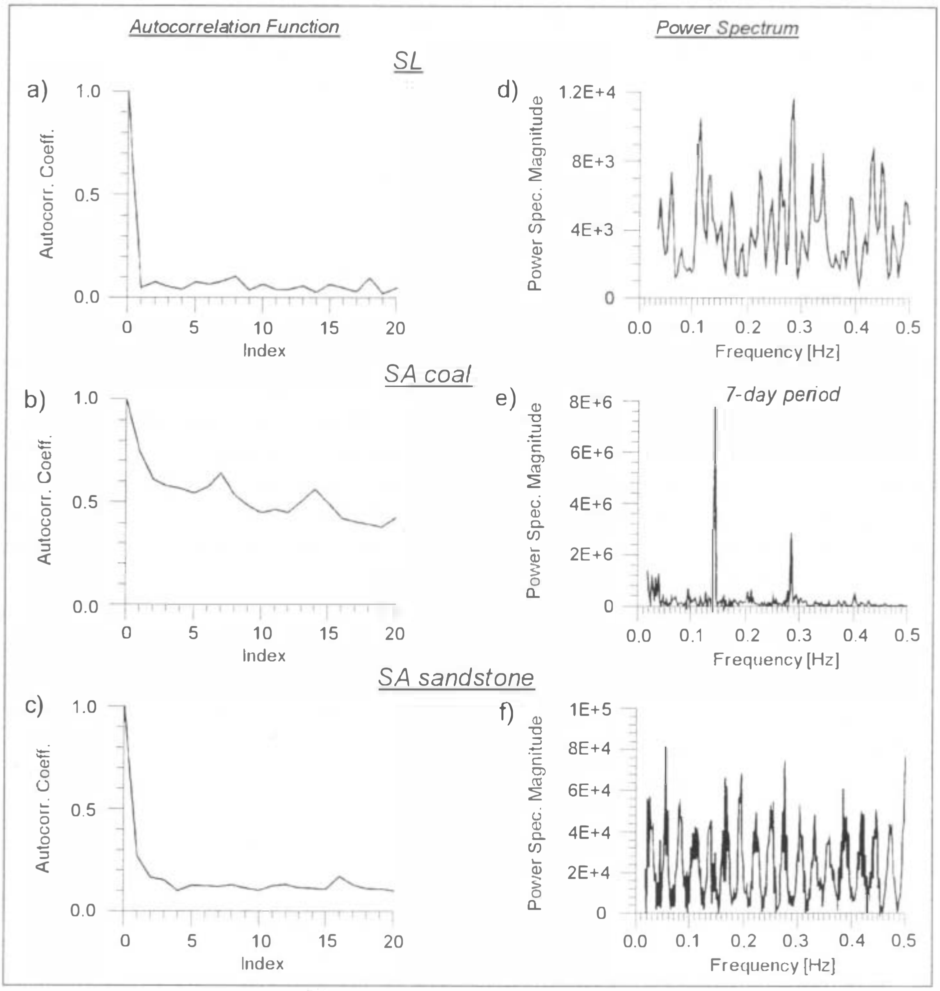

FIG. 9. Autocorrelation functions and power spectral densities for seismic released energy (SL) and seismoacoustic released energy in the coal and in the sandstone over coal seam.

1948 recorded events, and two criteria were used. On the basis of comparison of error prediction with long-term mean value (Masters, 1993):

$$\text{RMSE} = \frac{\sum_{i=1}^{N} (y_i - x_i)^2}{\sum_{i=1}^{N} (x_i - \overline{x})^2},$$

where y_i is the predicted value, x_i is measured value and $\overline{x}$ is the mean value of measured data and N is number of elements of both sets and on the bases of comparison of prediction with monitored time series final value prediction (i.e. number of events or the released energy will be the same the previous day as in the next):

$$\mathsf{LMSE} = \frac{\sum_{i=1}^{N} (y_i - x_i)^2}{\sum_{i=1}^{N} (x_i - x_{i-1})^2}.$$

Fig. 10a) graphically illustrates prediction results of seismic event number per day and Fig. 10b) results of SA event prediction recorded at coalface. From the size of RMSE and LMSE prediction error it is obvious that the predicted value of seismic and seismo–acoustic events is better than the mean by about 75 % and better than last value by about 40 %. For prediction of energy square root sums per day (Fig. 10c) the prediction is about 30 % better than the mean and about 40 % better than the last value. But prediction of strong events in predicted part of set of sums of energy square roots was not successful.

Analyses of several selected stronger events and their relation to blasting — time difference between blasting and development of a stronger event and focus distance from the coalface — reveals that events with focus in coalface vicinity of approx. 20 – 30 m above the coal seam (see Table 1) are influenced by blasting the most. This blasting distance is not sufficient to eliminate strong events developed in more distant overburden strata.

Table 1. Dependencies between selected strong induced seismic events and blasting.

	Blasting	Strong tremor	Time difference [day]	Altitude [m]
1	7.10.95	20.10.95	13	40
2	3.12.95	12.12.95	9	60
3	**17.3.96** **21.3.96**	**21.3.96**	**4** **0**	**12**
4	6.10.96	12.10.96	6	60
5	28.10.96	30.10.96	2	580
6	10.11.96 17.11.96	16.11.96 17.11.96	6 6	24 60
7	25.5.97	4.6.97	10	40
8	**4.5.97**	**4.5.97**	0	**20**
9	**9.6.97**	**9.6.97**	0	**10**
10	19.7.97	11.8.97	23	280

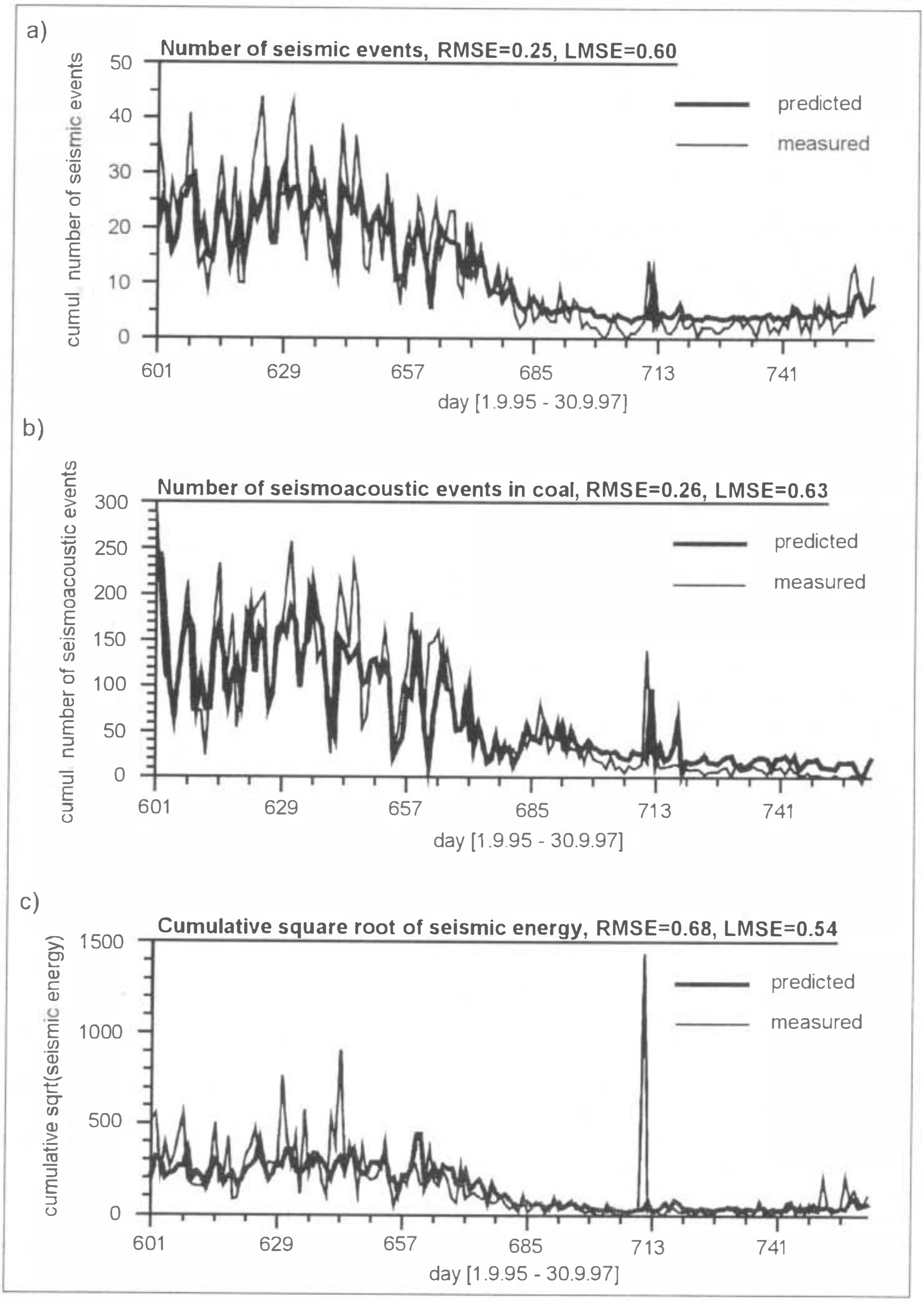

FIG. 10. Predicted and measured time series.

Conclusion

When mining coalface No. 14736, 44 energetically significant strong events in total, two (2) with energy bigger than 10^6 J, three (3) with energy bigger than 10^5 J and thirty nine (39) with energy bigger than 10^4 J, were recorded. Excluding these events 281 events with energy in order of 10^3 J was recorded. During the entire mining period active and passive elements of anti–tremor prevention were applied. Active measures affected rock mass properties and changed its stress conditions. They include wetting of coal pillars, distress blasting in coal and no break blasting in overburden of the coalface. All these measures resulted in continuous changes of the rock mass stress condition and contributed to the successful prevention. Although they did not stop mining tremors they contributed to no problem coalface mining. On the basis of local prognosis method in particular seismo–acoustic and seismological monitoring, introduction of these measures during the mining process was constantly adjusted according to the methodological procedure used in Ostrava – Karviná District. However, these interventions significantly influence input data of neural networks and consequently input series, include data regarding the rock mass reaction in relatively uniform mining and are influenced by outside interventions. This is the reason why before development of strong induced seismic events only significant characteristic changes in rock mass cannot be detected. During the mining period all five (5) significant events were localized relatively far from the coal seam but recording of SA emission data was done only in coal seam or its nearest overburden. For these reasons development of these strong events could not be estimated successfully and application of neural networks to determine the strong tremors development time was not very successful either. To gain data from vicinity of development of strong event focuses it would be necessary to position SA sensors in higher levels of overburden.

Acknowledgement: This study was performed under Grant No.: 105/96/1065, of the Grant Agency of the Czech Republic.

References

Holub K.: 1995, Preliminary Results of *b*–value analysis for Mining–Induced Seismic events. *Acta Montana* **A6** (95), 27–31.

Holub K., Veselá V.: 1995, Seismic Monitoring of the Longwall Face No. 138 704 at the Lazy Mine, *Acta Montana* **A6** (95), 43–51.

Kalenda P.: 1996, A Contribution to Discussion on Lower Limitation of Energy-Frequency Distribution. *Acta Montana* **A9** (100), 131–138.

Rudajev V., Lokajíček T., Číž R.: 1996, Structure Elements of Rocks and Energy–Frequency Distribution of Seismic Phenomena, *Acta Montana* **A9** (100), 121–130.

Číž R., Rudajev V.: 1996, Prediction Methods Based on Multichannel Statistical Extrapolation and their Application on Induced Seismic Events. *Acta Montana* **A10** (102), 133–144.

Rudajev V., Číž R.: 1998, Estimation of Mining Tremor Occurrence by Using Neural Networks. *Pure appl. geophys.* **154**, 57–72.

Masters T.: 1993, *Practical Neural Networks Recipes in C++*, Academic Press, San Diego CA.

Rumelhalt D.E., Hilton G.E., Wiliams R.J.: 1986, Learning Representations by Back–Propagating Errors, *Nature* **323**, 533–536.

Slavík J., Kalenda P., Holub K., Sglunda R.: 1989, Automatizace vyhodnocovacích postupů při vyšetřování seismické aktivity v OKR. *Acta Montana* **81**, 115–126.

Analýza časových řad akustické emise a důlních otřesů z oblasti Ostravsko–karvínských otřesových dolů

R.Číž, J.Holečko a V.Rudajev

V období od 8.9.1995 do 31.7.1997 probíhala na Dole Československá armáda těžba v porubu 14736, který byl zařazen do 3. stupně (nejvyššího) nebezpečí vzniku důlních otřesů. Na základě tohoto zařazení porubu byla prováděna systematická seismoakustická měření v lokalitě porubu a zároveň probíhal nepřetržitý seismický monitoring dané oblasti.

Seismoakustická měřicí síť byla sestavena z 5–7 snímačů, jejichž umístění se měnilo v závislosti na postupu porubu. Jeden z akustických snímačů byl vždy umístěn do nadloží ve vrtu cca 5 m dlouhém, ostatní snímače byly umístěny v uhelné sloji (zpravidla vždy dva na každé porubní chodbě). Pásma propustnosti SA snímačů byly v rozmezí 70 Hz až 2 kHz.

Seismická měření probíhala ve frekvenčním pásmu 1–50 Hz. Interpretace získaných dat se skládala především ze sledování změn četnosti akusticky registrovaných signálů i seismických dějů, zároveň byla vyhodnocována energie seismických dějů i prostorová migrace ohnisek. Použité sítě (Slavík a kol., 1989) umožňovaly lokaci ohnisek s dosti dobrou přesností v horizontální rovině, řádově desítky metrů. Vertikální složka polohy ohniska je zatížena větší chybou, avšak umožňuje relativně ocenit rozdílnou výšku registrovaných seismických jevů.

Takto získané údaje vytvářely databázi vhodnou pro použití protiotřesových opatření (zejména aplikaci trhacích prací, k omezení rychlosti dobývání, resp. i k zastavení práce na porubu). Cílem tohoto příspěvku je zpracovat zaregistrovaná data pomocí vícekanálových statistických extrapolačních metod a zdokonalit prognózu vzniku budoucího seismického děje.

Za celé období bylo seismickou sítí zaregistrováno 9280 dějů. Bylo prokázáno, že děje se nevyskytují rovnoměrně v čase, což bylo prokázáno uvolňováním energie v čase (obr. 1). Na základě průběhu uvolňování energie lze celé období rozdělit do 5 etap. Doba trvání těchto etap je omezená vždy výskytem silného seismického děje. Pro všechny etapy byly určeny energeticko–četnostní distribuce (EČD), přičemž pro IV. etapu, ve které nebylo zjištěno rovnoměrné uvolňování seismické energie, byla tato distribuce určena pro 3 dílčí intervaly, které jsou charakterizovány jinou směrnicí dE/dt a jiným množstvím celkové uvolněné seismické energie. Výsledky těchto analýz jsou na obr. 2 a 3. Všechny získané EČD mají prakticky stejný tvar, tj. v oblastech nižších energií je podstatně menší počet dějů, než by odpovídalo negativně–exponenciální distribuci a od jisté energie (40 J), tzv. charakteristické hodnoty (Holub, 1995; Holub a Veselá, 1995; Kalenda, 1996; Rudajev a kol., 1996), směrem k vyšším energiím lze distribuci popsat logaritmickým negativně–exponenciálním vztahem

$$\log(N) = a - b \cdot \log(E) \, .$$

Výsledky lokací ohnisek jsou znázorněny na obr. 4, kde opět celá doba dobývání porubu je rozdělena do výše definovaných etap. Za celé období bylo pozorováno celkem 5 dějů, jejichž energie přesáhla 10^5 J. Tři z těchto dějů lze klasifikovat jako důlní otřesy, neboť měly makroseismické účinky v důlním díle. Silný seismický jev z 4.6.1997 byl bez projevů v důlním díle, lze usuzovat, že pochází z vyššího nadloží.

Seismoakustický měřicí systém umožňoval registraci četnosti impulsů a ocenění jejich energie. Za celé období ražby bylo celkem zaregistrováno více než 85000 seismoakustických impulsů. Z hlediska lokace byly impulsy rozděleny na impulsy vzniklé ve sloji a impulsy vzniklé v nadloží.

Za účelem predikce seismických dějů byla využita metoda neuronových sítí, založená na nalezení nelineárních vazeb mezi jednotlivými posloupnostmi měřených veličin. Extrapolace seismické aktivity byla řešena pomocí rovnoměrné sítě s algoritmem učení backpropagation s momentem. Princip spočívá v tom, že síť je v první fázi "učena" na učící množině — dochází k optimálnímu nastavení vah podle vztahu (Rumelhalt, 1986; Číž, Rudajev, 1996; Rudajev, Číž, 1998):

$$\triangle w_{ij}^{(t)} = -\eta \frac{\partial E}{\partial w_{ij}} \left(\vec{w}^{(t)} \right) + \alpha \triangle w_{ij}^{(t-1)} ,$$

kde $\triangle w_{ij}^{(t)}$ označuje změny vah po iteračním kroku t, $\frac{\partial E}{\partial w_{ij}} (\vec{w}^{(t)})$ označuje gradient energetické funkce, η je parametr učení a α označuje moment. Po adaptaci vah sítě v další fázi jsou na vstup předkládány nové vzory a výstupem je požadovaná hodnota parametru v budoucím čase.

Vstupní řady byly rozděleny na dvě části — učící množina měla 600 prvků posloupnosti a za tuto dobu bylo zaregistrováno 7332 dějů. Na těchto učících řadách byly stanoveny parametry neuronové sítě, která měla 1 skrytou vrstvu se třemi skrytými neurony, což se na základě dřívějších testů jeví jako dostatečné (Rudajev, Číž, 1998). Úspěšnost predikce byla testována na množině predikovaných hodnot, která měla 161 prvků posloupnosti a byla vytvořena z 1948 registrovaných dějů, přičemž byly použity 2 kritéria. Na základě porovnání chyby predikce s dlouhodobou střední hodnotou RMSE a na základě porovnání predikce s predikcí poslední LMSE.

Výsledky predikce počtů seismických dějů za den jsou graficky znázorněny na obr. 10a) a výsledek predikce SA dějů zaregistrovaných v porubu na obr. 10b). Z velikosti chyby predikce RMSE a LMSE vyplývá, že predikovaná hodnota počtu seismických i seismoakustických dějů je lepší než střední hodnota o asi 75 % a lepší než poslední hodnota o asi 40 %. Pro predikci součtu druhých odmocnin energií za den (obr. 10c) je predikce lepší asi o 30 % než střední hodnota a o 40 % lepší než poslední hodnota. Neúspěšná však byla predikce silných dějů v predikované části řady součtu odmocnin energií.

Z analýzy několika vybraných silnějších dějů a jejich závislostí na trhací práci — časovou diferencí mezi trhací prací a vznikem silnějšího děje a vzdálenosti ohniska od porubu — uvedených v tabulce 1 je patrné, že nejvíce jsou trhacími pracemi ovlivněny děje, které mají své ohnisko v blízkosti porubu do cca 20–30 m nad slojí. Dosah trhacích prací není zcela dostatečný pro eliminování silných dějů pocházejících ze vzdálenějších nadložních vrstev. Tyto zásahy však výrazně ovlivňují vstupní data do neuronových sítí. Všech pět významných dějů za období ražby bylo lokalizováno do větší vzdálenosti od uhelné sloje, avšak získání údajů SA emise bylo prováděno pouze v uhelné sloji, resp. jejím nejbližším nadloží. Z těchto důvodů nebylo možné úspěšně odhadnout vznik těchto silných jevů. Pro získání informací z blízkosti oblastí vzniku ohnisek silných jevů by bylo potřeba umístit SA snímače ve vyšších patrech v nadloží.